Laboratory Evaluation of Magnetic Flux Forces Generated by Active Magnetic Bearings - Type A and Type B

Marcelo CARVALHO*, Afonso DEL NERO GOMES*, Antonio FERREIRA*, Domingos DAVID**, José SANTISTEBAN**
*Federal University of Rio de Janeiro, Brazil
** Federal University Fluminense, Brazil

1. Introduction

Four poles active magnetic bearings (AMB) have been discussed in the literature for more than ten years [2] [3]; and the magnetic poles flux distribution, analyzed per finite elements method (FEM) for the comparison between the type A [4] and type B [5] AMB already known. Now, the magnetic core bearing reluctance variation under balanced and unbalanced currents can be combined, simultaneously with mechanical offsets to the centered position; and then, may be simulated by FEM. Identifying what type of active magnetic bearings produces stronger forces to center the motor axis, such as mechanical bearings do, improves efficiency to the control magnetic fields at reduced inductances and electrical currents can be simulated and calculated. Finally, the consideration of S. J. Salon [6] that some calculation methods may not be "completely reliable" is the object of investigation of this work, which compares the simulated method results with actual laboratory static and dynamic measurements of on AMB type A and type B prototypes, .

2. Study objective

In this study, FEM is used to estimate the magnetic forces applied to a type A and B active magnetic bearing. The geometries were carefully selected, in order to allow the comparison between the simulated FEM values with the actual forces applied to two prototypes, with architectures corresponding to type A and type B AMB, with same geometries, in a laboratory. Two methods were choosen, one static, measuring forces with bias current and another dynamic, with the motor running applying unbalanced weight to the axis of the motor. The values obtained by the simulation and the laboratory tests are the subjects of analysis.

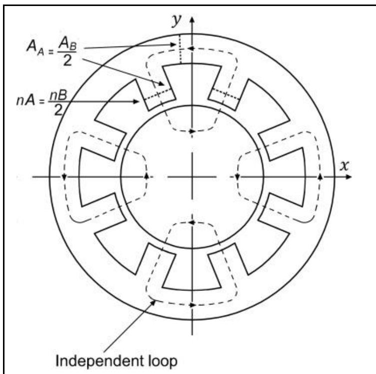

Fig. 1 - Eight teeth AMB

The type A AMB (Fig. 1) consists of eight electromagnets arranged in pairs, two sets disposed horizontally (x, x') and two vertically (y, y'). The four independent magnetic flux loops controls the AMB position.

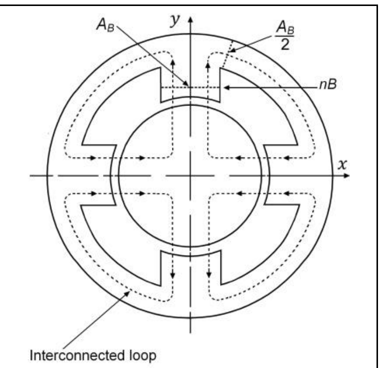

Fig. 2 - Four teeth AMB

The type B AMB (Fig. 2) consists of four electromagnets, disposed horizontally (x, x') and vertically (y, y'). The four interconnected magnetic flux loops controls the AMB position.

Both architectures employ two pairs of proximity sensors, aligned with the axis x and y in order to provide the feedback control with the dynamic position of the motor axis at any time.

Prototype construction:

Section A_A area is half of the area of section A_B; the number of windings of the coils on Type B AMB (nB) teeth have twice the number of windings of coils in Type A AMB teeth $(2 * nA)$. (Figs 4 and 5, AMB Prototypes).

The electrical currents fed to the AMB coils on both prototypes are $I_0 \pm i_x(t)$, and $I_0 \pm i_y(t)$, where I_0 is the bias current, while the differential currents i_x and i_y control the rotor position.

The resultant forces [1] f_x^a, f_y^a, f_x^b and f_y^b, can be expressed in terms of $I_0 \pm i_x(t)$ and $I_0 \pm i_y(t)$

The number of coils nA - nB; the cross sections areas in the ferromagnetic material A_A - A_B; and the air magnetic permeability μ_0 and nominal lengths h of the air gaps, which are the same for both AMB prototypes (type A and B -Fig. 1 and Fig. 2) [2] allow the calculation of the magnetic forces (1) (2).

$$\left.\begin{aligned} f_x^a &= k_p^a x + k_i^a i_x \\ f_y^a &= k_p^a y + k_i^a i_y \end{aligned}\right\} \text{where} \left\{\begin{aligned} k_p^a &= \mu_0 A_a n_a^2 I_0^2 / h^3 \\ k_i^a &= \mu_0 A_a n_a^2 I_0 / h^2 \end{aligned}\right. \quad (1)$$

$$\left.\begin{aligned} f_x^b &= k_p^b x + k_i^b i_x \\ f_y^b &= k_p^b y + k_i^b i_y \end{aligned}\right\} \text{where} \left\{\begin{aligned} k_p^b &= 2\mu_0 A_b n_b^2 I_0^2 / h^3 \\ k_i^b &= 2\mu_0 A_b n_b^2 I_0 / h^2 \end{aligned}\right. \quad (2)$$


Fig. 3 – External View

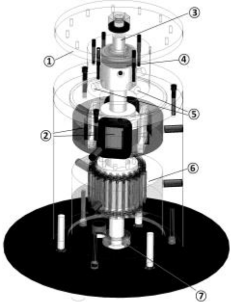

(1) Balance Wheel
(2) AMB
(3) Shaft
(4) Safety bearing
(5) Position sensor's pit
(6) Motor
(7) Compensation bearing

Fig. 4 – Exploded View


Fig. 5 - Type A Internals


Fig. 6 -- Type B Internals

AMB Prototype

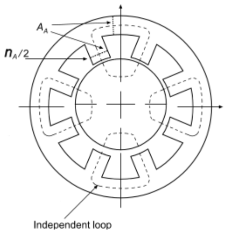

Fig. 7 -

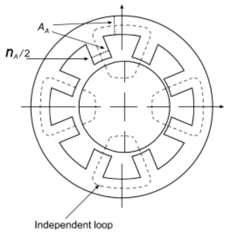

Fig. 8 –

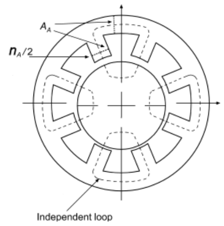

Fig. 9 –

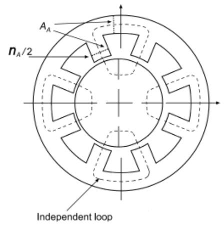

Fig. 10 –

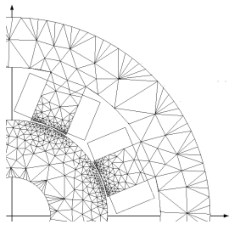
Fig. 11 –

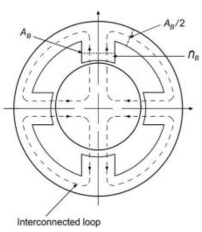

Fig. 12 -

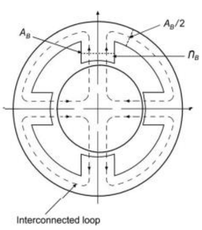

Fig. 13 –

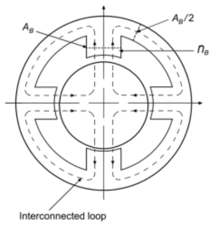

Fig. 14 –

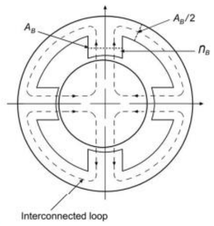

Fig. 15 –

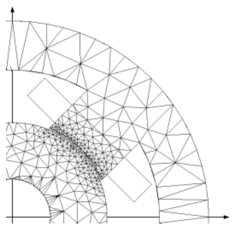
Fig. 16 –

FEM AMB Type A (Figs. 7 to 11) and AMB Type B (Figs. 12 to 16) simulations are run for different offset positions and same conditions are applied to the prototype, for static forces applies to the axis Y measurements. Dynamic tests will be shown with the motor spinning and unbalanced masses applied to the motor wheel (Fig. 3).

References

[1] Schweitzer G., Bleuler H., Traxler A. (1994), Active Magnetic Bearings, Hochschulverlag AG and der ETH Zuerich

[2] David D. F. B., Santisteban J. A., Del Nero Gomes A. C. (2017), Modeling and Testing Strategies for an Interconnected Four-Pole Magnetic Bearing, Actuators 6, no. 3: 21. https://doi.org/10.3390/act6030021

[3] David D. F. B., Santisteban J. A., Del Nero Gomes A. C. (2014), "Interconnected Four-Pole Magnetic Bearing Simulations and Testing", ISMB14, 14th International Symposium on Magnetic Bearings.

[4] Pabitra K. Biswas, Subrata Banerjee (2013),"ANSYS Based FEM Analysis for Three and Four Coil Active Magnetic Bearing-a Comparative Study", International Journal of Applied Science and Engineering, 277-292

[5] David D. F. B., Santisteban J. A., Del Nero Gomes A. C. (2017), "Modeling and Discussing an Interconnected Flux Magnetic Bearing", ACES JOURNAL, Vol. 32, No. 8.

[6] S. J. Salon, (1995), "Finite Element Analysis of Electrical Machines", DOI 10.1007/978-1-4615-2349-9, Springer Science+Business Media, New York, USA